Journal of Molecular Graphics and Modelling 30 (2011) 100–109

Contents lists available at ScienceDirect

Journal of Molecular Graphics and Modelling

journal homepage: www.elsevier.com/locate/JMGM

Discrimination of agonists versus antagonists of nicotinic ligands based on docking onto AChBP structures

Antoine Taly[a,*], Claire Colas[b], Thérèse Malliavin[b], Arnaud Blondel[b], Michael Nilges[b], Pierre-Jean Corringer[c], Delphine Joseph[d]

[a] Laboratoire de Conception et Application de Molécules Bioactives, UMR 7199 CNRS-Université de Strasbourg, 74 Route du Rhin – BP 60024, 67401 Illkirch Cedex, France
[b] Unité de Bioinformatique Structurale, Institut Pasteur et URA CNRS 2185, 25-28 rue du Dr Roux, F-75724 Paris Cedex 15, France
[c] Groupe à 5 ans Canaux-Récepteurs, CNRS URA 2182, 25-28 rue du Dr Roux, F-75724 Paris Cedex 15, France
[d] University Paris-Sud, Equipe de Synthèse Organique et Pharmacochimie de Composés d'Intérêt Biologique, UMR CNRS 8076 BioCIS,5 rue Jean-Baptiste Clément, F-92296 Châtenay-Malabry Cedex, France

ARTICLE INFO

Article history:
Received 14 January 2011
Received in revised form 27 May 2011
Accepted 22 June 2011
Available online 29 June 2011

Keywords:
Nicotinic acetylcholine receptor
Drug design
Virtual screening

ABSTRACT

Numerous high-resolution crystallographic structures of the acetylcholine binding protein (AChBP), a molluscan cholinergic protein, homologous to the extracellular domain of nicotinic acetylcholine receptors, are available. This offers opportunities to model the interaction between various ligands and the acetylcholine binding site. Herein we present a study of the interplay between ligand binding and motions of the C-loop capping the binding site.

Nicotinic agonists and antagonists were docked on AChBP X-ray structures. It is shown that the studied agonists and antagonists can be discriminated according to their higher affinities for structures respectively obtained in the presence of agonists or antagonists, highlighting the fact that AChBP structures retain a pharmacological footprint of the compound used in crystallography experiments. A detailed analysis of the binding site cavities suggests that this property is mainly related to the shape of the cavities.

1. Introduction

Nicotinic acetylcholine receptors (nAChRs) play a central role in intercellular communications in the brain and at neuromuscular junctions. The nAChRs mediate cholinergic signal transmission through the postsynaptic membrane at the neuromuscular synapse (reviewed in [1]). The receptors are involved in cognitive processes, such as attention, access to consciousness, learning and memory and their pathologies include nicotine addiction, autism, schizophrenia, Parkinson and Alzheimer's disease [2]. Understanding the functional organization of the nAChRs at the atomic level can provide useful insights for the development of new drug therapies [3].

The nAChRs are members of the Cys-loop superfamily of ligand-gated ion channels. They are pentameric integral membrane proteins with a fivefold pseudo-symmetry axis perpendicular to the membrane. Each subunit consists of an extracellular domain (ECD) containing the ligand binding site and a transmembrane ion pore domain (IPD). The acetylcholine (ACh) binding site in the ECD is at the boundary between subunits (Fig. 1a and b) and the IPD delineates an axial cation-specific channel [4,5]. The topologically distinct ECD and IPD are allosterically coupled to each other [6]. Thus, nAChRs have the necessary structural elements to convert a chemical signal, typically a local increase in extracellular ACh concentration, into an electrical signal generated by the opening of the ion channel.

Electrophysiological analysis of nAChRs shows that rapid delivery of ACh promotes fast opening of the channel, and that a prolonged application leads to a slow decrease of the response amplitude or "desensitization". It is generally assumed that there is a reversible equilibrium between a basal state with closed channel (B), an active open channel state (A), and one or several high affinity desensitized state(s) with a closed channel (D) (see [1,7]). The nAChR can activate in the absence of ligand [8,9]. But, nAChR ligands act according to their affinities for these different states, stabilizing the conformation for which they have the highest affinity: antagonists display a higher affinity for the basal (or desensitized) state whereas ACh and nicotinic agonists have a higher affinity for the active (and desensitized) state(s).

The acetylcholine binding protein (AChBP) from the fresh water snail *Lymnea stagnalis* [10,11] provided the first structure available to interpret the conformation of nAChRs. This protein has been proposed to participate in a buffering activity, modulating the concentration of ACh in the mollusc's synapses [12]. In addition to its

* Corresponding author.
E-mail address: a.taly@unistra.fr (A. Taly).

1093-3263/$ – see front matter © 2011 Elsevier Inc. All rights reserved.
doi:10.1016/j.jmgm.2011.06.008

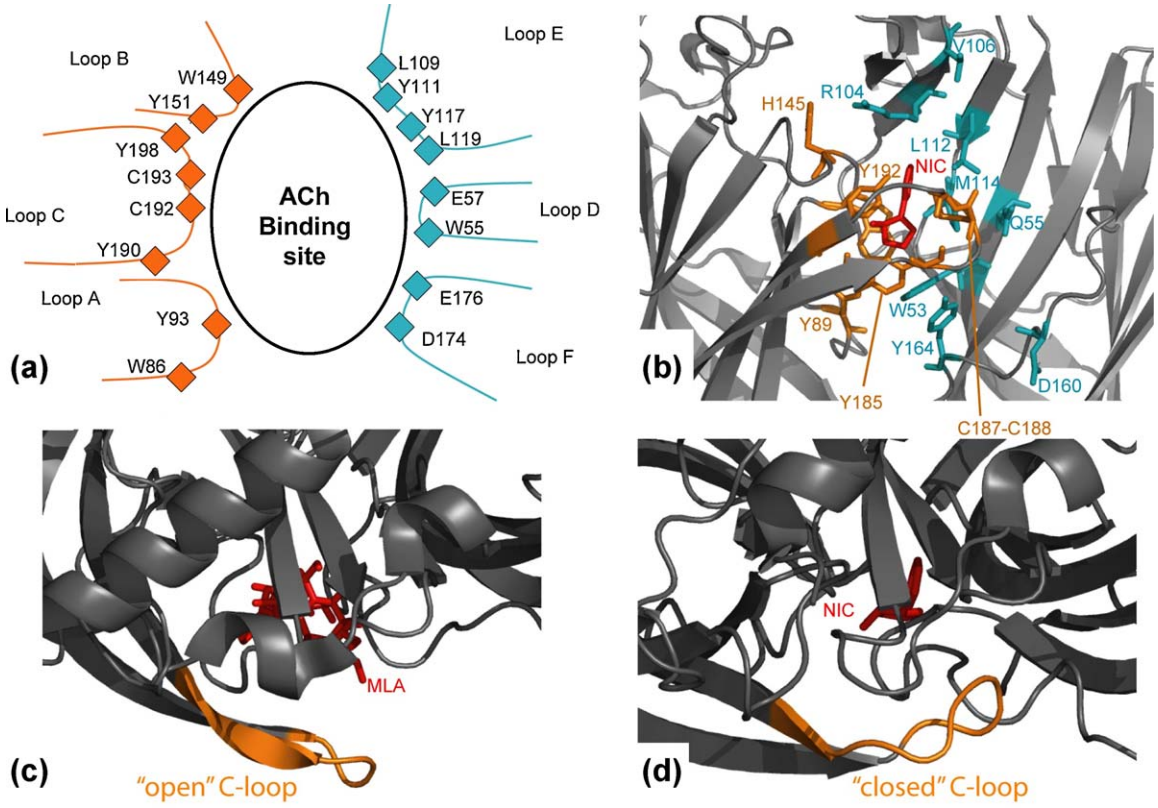

Fig. 1. AChBP structures and binding site. (a) Residues essential for ligand binding identified by mutagenesis studies [3]; (b) nicotine bound to AChBP and surrounding residues, homologous to those displayed in (a); (c) MLA bound to AChBP viewed from top (PDB code: 2BYR); (d) nicotine bound to AChBP viewed from top (PDB code: 1UW6). Panels (c) and (d) allow seeing the conformational change related to antagonist versus agonist binding. In particular, it is seen that in the presence of MLA the b-strands are longer and the C-loop is in an "open" configuration.

function related to those of nAChRs, AChBP forms homopentamers and has a significant sequence homology of roughly 30% with the ECD of the nAChRs. Moreover, the residues of the binding site are remarkably conserved between AChBP and nAChRs (panels a and b of Fig. 1). Consequently, the structure of AChBP has been exploited to derive models of the ECD of nAChRs [13]. Use of AChBP has also been proposed for drug design projects aimed at developing nicotinic agonists [14].

AChBP structures have also been employed to infer conformational changes of the nAChR upon ligand binding. An analysis of all known AChBP conformations revealed only two categories, either "open" or "closed" defined by the conformation of the C loop that caps the binding site [15]. Interestingly, all structures corresponding to the basal state display an "open" C-loop whereas the others have a "closed" loop C [15] (Fig. 1c and d). It was noticed later that (i) structures bound to partial agonists show a more complex behaviour [16]; (ii) the "open" C-loop structures are different among them and some should rather be named "intermediate" (see for example the recently determined AChBP structures bound to phycotoxins [17]). Modelling studies suggested that the motion of the C-loop is coupled to a global motion involved in the opening of the ion channel in nAChRs, although the structure of the rest of the AChBP is rather unmodified upon ligand binding [18–23].

We studied AChBP because it is, up to now, the largest source of atomic resolution structures in the LGIC family, revealing binding poses of known agonists and antagonists of the nAChRs [24–27] and providing starting points for modelisation [13,28–44]. AChBP has also been used in docking studies [45–54]. It was for example shown that α-cobratoxin can bind only when the C-loop is open [54]. Interestingly, similar observations have also been made with models of nAChR based on AChBP [44,55].

This article aims to study the interplay between ligand binding and the motion of the C-loop. QSAR analyses point out that the ligand size is important to nicotinic pharmacophore definition, indeed among nAChR ligands, agonists tend to be small whereas antagonists are bulkier [56]. Furthermore, a recent study [57] shows that the ligand size can be used to predict the correct C-loop closure during the docking to AChBP proteins. In a previous study, we have shown that α-cobratoxin can be docked to AChBP or nAChR only when the C-loop is open [54]. Herein, we present the docking of nicotinic agonists and antagonists on AChBP X-ray structures using a protocol compatible with virtual screening of large compound libraries. It is shown that it is possible to differentiate between agonists and antagonists from docking results: most antagonists only fit to open C-loop conformations whereas agonists show higher affinity for closed C-loop ones. An original analysis, based on the calculation of the cavities at the dimer interfaces, also suggests that the ligand activity is related to the whole shape of this cavity.

2. Methods

2.1. Docking

Docking was performed with the Autodock program (suite 4) [58]. Each ligand was docked to each structure with default Autodock4 settings except that docking was repeated 100 times (instead of 10). This was done to test the robustness of the approach because the final binding mode may depend on the randomly chosen starting position and conformation of the ligand, especially for large ligands with numerous degrees of freedom. Results prone to artefacts are then detected by the clustering of the docking poses: i.e. they appear as outliers (see below).

The protein (AChBP) structures (PDB entries: 2BR7, 3C79, 2BYQ, 2BYP, 2WN9, 2C9T, 2BR8, 2UZ6, 2BYN, 2BYR, 2BYS [16,25,26,59–61]) were prepared with the script 'prepare_receptor4.py' of Autodock that assigns atomic partial charges and radii. Flexibility of the protein was included implicitly by performing the docking to X-ray structures of different AChBPs from the specie *Aplysia californica*. These structures were obtained in the presence of ligands identified as agonists or antagonists, or without ligands (apo pocket or pocket containing the buffer molecule, Hepes). Autogrid4 was used to generate docking grids centered on the nicotine binding pocket with default settings except that 60 points rather than 40 were used in each direction to encompass the whole binding site and to leave enough space to allow the docking of ligands outside the binding pocket.

The docking was performed on the dimers formed by chains A and B of each analysed structure. Clustering was done with Autodock based on a RMSD cut-off of 2.0 Å. A cluster was considered for further analysis when it contained at least three poses.

2.2. Ligands preparation

The known active ligands were common synthetic compounds and toxins acting on the nAChRs (Supplementary Figs. 1 and 2). In addition, synthetic antagonists identified from two recent works [62,63] are named accordingly Liu-28/48/66 and Zaveri-5. The structures were built in ChemDraw Ultra 9.0 and the basic nitrogen of each alkaloid was protonated according to physiological pH (pH 7.4). Tautomers for CAP-55, tropisetron, feruginine, nicotine, TC-1698 and MLA were all generated. The three dimensional (3D) atomic coordinates of these structures were generated using Chem3D Ultra 9.0 and the more stable conformation was calculated using an MM2 energy-minimization. The ligands were then prepared with the Autodock script 'prepare_ligand4.py' that assigns atom types and partial charges and defines rotational degrees of freedom.

2.3. NCI diversity set preparation

The NCI diversity set contains compounds developed against cancer. It is not expected to contain nAChR ligands and is used as a control.

This set was retrieved as a series of PDB files from the Autodock web-site (http://autodock.scripps.edu/ressources/databases). Files containing atom types not being parametrized in Autodock (Ni, Pt, Pd, Rh, Sn, Sb, Se, Co, Ag, Si, As, Au, Cr and Cu) were removed. Molecules with less than 6 heavy atoms were also removed. Files containing two molecules were edited to remove the smaller one. The resulting PDB files were then prepared with the Autodock script 'prepare_ligand4.py' as it was done for the other ligands.

2.4. Clustering of docking results

For each set of docking poses, the lowest energy cluster detected by Autodock (see above) was kept. The binding energies of ligands on the AChBP structures were used to cluster the structures using the respective energies RMSD as a distance. Similarly, ligands were clustered according to their binding energies on the receptors. The hierarchical clustering used hclust [79] available in the R software [80].

2.5. Ligand pocket analysis

Cavities located at the interface between monomers in AChBP were analysed on the 75 cognate dimers extracted from the crystal structures (PDB entries: 2BR7, 2BR8, 2BYN, 2BYP, 2BYQ, 2BYR, 2BYS, 3C79, 2WN9, 2C9T, 2UZ6). Those dimers were oriented by superimposition on chains A and B of 2BYP. The superposition was performed using the McLachlan algorithm [64] as implemented in the program ProFit [81].

Cavities were detected on each oriented dimer using a program developed in the "Unité de Bioinformatique Structurale". Cavities are defined on a 0.5 Å-spacing grid as the solvent accessible volume [65]. The protein atoms are represented as van der Waals spheres with the van der Waals radii of N, H, O, C and S atoms equal to 1.6, .6, 1.6, 2.3 and 1.9 Å respectively. The inner limit (facing the protein surface) of the cavities is determined by rolling a probe of 1.4 Å on the protein, whereas the outer limit (facing the solvent) is determined by rolling a probe of 10 Å. Cavities are then clustered by contact, based on the centre of the solvent sphere accessible volume.

The cavity capped by the loop C was selected manually among those generated automatically for each oriented dimer. The distance between cavities was calculated as the overlap fraction between grids. These fractions were used to perform a hierarchical clustering of the cognate dimers extracted from the PDB structures.

3. Results

Our studies were restricted to the specie *A. californica*. AChBP structures from *L. Stagnalis* were excluded because species specificities have been experimentally observed [14]. Besides, the limited number of available structures from this organism at the beginning of this study might have biased the analysis. The single structure from *Bulinus Truncatus* (2BJ0) was also excluded.

3.1. Comparison with experimental data

As a test of the methodology, we performed docking of the ligands observed in the AChBP crystal structures (Fig. 2). Agonists were Imidacloprid, 4OH-DMXBA, epibatidine, lobeline and were docked on the structures of AChBP with a closed C-loop (3C79, 2BR7, 2BYQ and 2BYS). MLA represented antagonists and was docked on the structures with an open C-loop (2WN9, 2BR8, 2BYP, 2BYR, 2BYN, 2UZ6 and 2C9T).

Affinity calculated for Imidacloprid, experimentally bound to 3C79, was between −7.04 and −7.97 kcal mol^{-1}. The clustering of ligand poses reveals that: the first cluster for structure 3C79, the second cluster for 2BYQ and 2BYS and the fourth one for 2BR7 (Fig. 2a) were superimposed to the ligand crystalline pose.

For 4OH-DMXBA, experimentally bound to 2WN9, the affinity varied in the −9/−10.36 kcal mol^{-1} range. The ligand poses were clustered: the first cluster for structure 2BYQ, 2BR7 and 3C79, and the second cluster for 2BYS (Fig. 2b) superimposed to the ligand crystal conformation.

The docking of lobeline, experimentally bound to 2BYS, only reproduces the X-ray pose for structure 2BYS (Fig. 2c). Indeed, the orientation of Tyr 91 of 2BYS is not reproduced in 2BYQ, 3C79 and 2BR7 and, consequently, docking poses different from that of the 2BYS crystal and weaker scores were obtained in 2BYQ, 3C79 and 2BR7.

Epibatidine, experimentally bound to 2BYQ, was found to dock in the same orientation as in the X-ray structure for structures 2BYQ, 2BR7 and 3C79 (Fig. 2d). It had a slightly modified orientation in 2BYS, due to the position of Tyr 91 but its cationic azabicyclic skeleton kept the crystal position. Affinity calculated for epibatidine was between −8.25 and −9.07 kcal mol^{-1}.

In the case of the antagonist MLA, the 2BYR X-ray binding mode was only reproduced within this structure (Fig. 2e). C-loop openings different from those of 2BYR produced nevertheless strong binding affinities, equivalent to the values found for 2BYR.

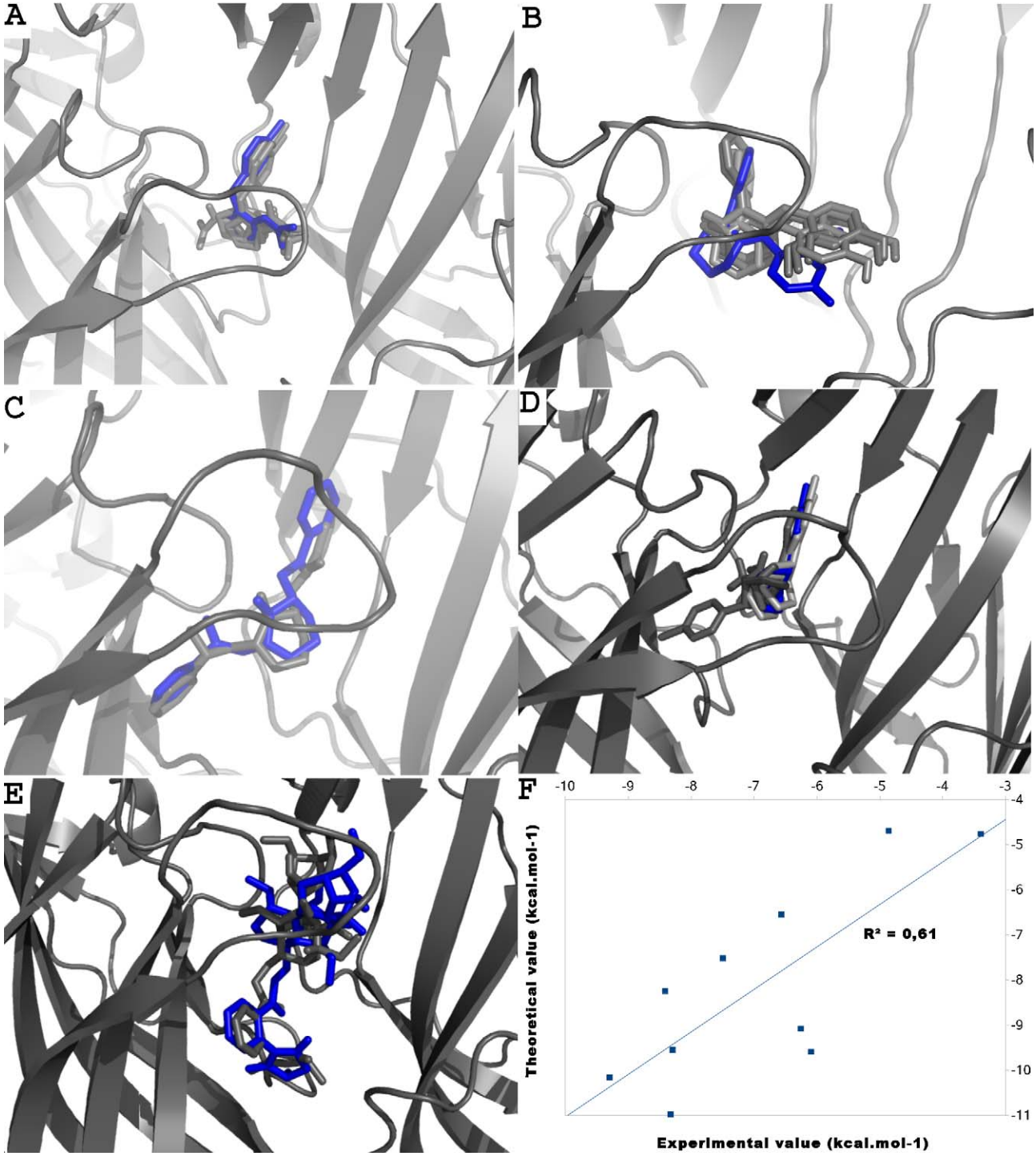

Fig. 2. Comparison of ligands docking and crystallographic poses. (a–e) Close view of the orthosteric binding site of AChBP. The ligands are drawn in stick representation with the crystallographic pose coloured in blue and the closest docking solution in grey. (a) Imidacloprid (experimentally bound to 3C79), (b) DMXBA (experimentally bound to 2WN9), (c) lobeline (experimentally bound to 2BYS), (d) epibatidine (experimentally bound to 2BYQ) and (e) MLA (experimentally bound to 2BYR). (f) Comparison between experimental and calculated binding energies (kcal mol^{-1}) of the ligands shown in (a–e).

In summary, the docking procedure mostly reproduced the binding mode of compounds observed in complexes solved by X-ray crystallography whatever AChBP X-ray structure used. In all cases, the docking binding energy was better than −4.1 kcal mol^{-1}. Furthermore, the crystal binding pose was always ranked in the top 4 poses, with a docking score close to the best one.

The quality of Autodock binding energies was assessed by comparing them to the experimental affinities on AChBP measured for the compounds tested here (Imidacloprid, 4OH-DMXBA, epibatidine, lobeline and MLA; Supplementary Table 2) [26,66,67]. The comparison reveals (Fig. 2f) a significant correlation (R^2 = 0.61) and further supports the docking procedure.

3.2. Docking of known agonists and antagonists on various AChBP structures displaying open/closed C-loop

The tests presented above insured that the docking protocol correctly reproduced the binding mode of compounds found in

crystallographic complexes. The next step was to test the binding difference between agonists and antagonists on the different structures. Antagonists were anticipated to better bind to structures obtained in the presence of antagonists while agonists were expected to better bind to structures bound to agonists. Therefore, we built a small virtual library of agonists and antagonists (see Section 2 for the details and Supplementary Figs. 1 and 2 for their structures) and docked them on the AChBP structures. The compounds were chosen in order to maximize the chemical diversity of the library and therefore, in addition to drugs, include toxins [68].

The docking results are reported in Supplementary Table 1. The binding affinities difference between docking poses can be magnified by plotting, for each ligand, its affinity to a given structure versus the affinity difference with other structures. For example, Autodock affinity difference between the structures 2BYQ (bound to epibatidine) and 2BYR (bound to MLA) plotted versus the affinity for structure 2BYQ (Fig. 3a) showed that agonists (black bullets) were located in the range −0.1/0.0 of the *Y* axis and thus displayed similar affinities for both structures with a slightly higher affinity for 2BYQ. Antagonists (white bullets) display a contrasted behaviour. Large antagonists were mainly located in the range of positive values of axis *Y*, and thus had a higher affinity for 2BYR, whereas small-size antagonists were more similar to agonists and display similar affinity for 2BYQ and 2BYR. The larger affinity difference observed for large antagonists (see for example MLA in Supplementary Fig. 3) is observed because these ligands do not fit inside the binding site when the C-loop is closed.

The docking affinity patterns observed for agonists and antagonists on various structures (Supplementary Table 1) were used to perform a clustering of the ligands. The profile of binding energies of each ligand on all AChBP structures permits to calculate an energy RMSD between ligands, used as a distance for hierarchical clustering (for details see Section 2). Bulky antagonists (MLA, pancuronium, vecuronium, rocuronium, tubocurarine, and lophotoxin) formed a well-separated group, distant from the agonists and the small antagonists (Fig. 3c).

Similarly, all protein structures used for the docking were clustered as a function of their affinity pattern for the agonists and antagonists (see Section 2) (Fig. 3b). The structures determined in the presence of antagonists formed a group distinct the structures bound to agonists. Together these results suggested that docking could reveal the activity of a ligand, agonist versus antagonist, and the pharmacological footprint of structures.

The observed exception, i.e. small antagonists clustered with agonists, is noteworthy. This might be related to the fact that the small antagonists stabilize the desensitized state rather than the basal state, as it has been proposed for DHβE [69]. As this trend may also be due to the relatively small size of these antagonists, we decided to study the influence of the ligand size and of the interface cavity volume for the docking in various AChBP structures.

3.3. Role of the size of the ligand and of the interface cavities

The influence of the ligand size on the docking was analysed independently of possible ligand affinity for nAChRs. This was done using the large NCI diversity set of compounds provided with Autodock (see Section 2). As this set was produced for cancer studies, it is expected to be "neutral" as far as binding to AChBP is concerned.

The docking affinity for 2BYQ (bound to epibatidine) was compared to the affinity difference between 2BYQ and 2BYR (bound to MLA) structures (Fig. 4a and b). Total affinity (Fig. 4a) and affinity per heavy atom (Fig. 4b) were analysed, and two groups are detected in both cases. The affinity difference was then analysed as a function of size (Fig. 4c and d) and reveals a pattern similar to what was observed for nicotinic compounds (Fig. 3a). Indeed, most of the largest compounds containing more than 30 heavy atoms (Fig. 4d) showed a higher affinity for 2BYR, while smaller compounds (Fig. 4c) display similar affinities for 2BYR and 2BYQ. Thus, in agreement with the observations made on nicotinic compounds, small compounds fit inside the binding site whereas bigger ones were partly or totally outside of the binding pocket.

In order to complement the ligand size analysis, the geometry of the cavity containing the ligand binding pocket was explored as described in Methods. The size of the cavities ranged from 100 to 10,000 grid points. The smallest cavities were capped by the closed C loop of AChBP structures bearing agonists (Fig. 5a). The largest cavities covered the orthosteric pocket, located under the C loop, but spread beyond the binding pocket limits over the whole subunit interface (Fig. 5b). The only biological information used to define the calculated cavities was its location behind the C-loop. Thus, they did correspond neither to a pharmacological, nor to a pharmacophoric definition, but rather to a purely geometric one.

Superimposition of the cavities calculated for the 75 dimers extracted from the AChBP crystal structures and hierarchical clustering of them (Fig. 5c) partitioned the cavities in two main groups. Group 1 contained the interfaces binding nAChR-agonists, epibatidine and imidacloprid and lobeline. Remarkably, lobeline cavity (2BYS) formed a separate cluster, in agreement with the docking results (see above). Group 2 contained the interfaces binding antagonist ligands the partial agonist 4OH-DMXBA, crystallographic factors and apo structures.

A closer inspection of the clusters revealed that dimers from the same PDB structures belonged to the same cluster. There are three exceptions to this rule. First, apo interfaces (in black) and interfaces bound to the crystallization buffer molecule (in blue) are dispersed among all the clusters. This is in agreement with the observed flexibility of the C-loop in absence of ligand [70]. Second, the five antagonist-bound interfaces of each structure 2C9T and 2BYP partition in both 3a and 3b groups. This common partition in two clusters is an interesting finding as they are complexed with the same ligand: α-conotoxin IMI. Hence this shows that a common structural binding mode lead to a common classification of the cavities. A third exception is the dispersion of the 2WN9 cavity bound to 4OH-DMXBA among the groups 2a, 3a and 3b, containing antagonist-bound cavities. The classification with antagonists agrees with the activity pattern of the partial agonist 4OH-DMXBA, which should be intermediate between agonist and antagonist activity patterns. The dispersion of the 2WN9 cavities in the clustering agrees with the variability of C-loop conformation noticed in the crystallographic structure [16].

The hierarchical clustering of the cavities detected at dimer interfaces, allowed to detect homogeneous groups of antagonist and agonist-bound interfaces. Both groups included interfaces bound to crystallographic co-factors.

The same hierarchical clustering was performed on the cavities involved in the docking reported in Fig. 3b (formed by subunits A and B, Supplementary Fig. 4, left). In addition, those cavities were also clustered using the difference in volume as opposed to the overlap fraction as a distance (Supplementary Fig. 4, right). The dendograms of the docking energies (Fig. 3b) and of the cavities volume (Supplementary Fig. 4, right) and overlap (Supplementary Fig. 4, left) discriminate between agonist and antagonist-bound AB dimers. Nevertheless, the dimer AB bound to HEPES (2BR7) is clustered with agonists if the docking energies or the cavities volume are used as distance, whereas this dimer forms an isolated cluster in the dendogram based on the cavities overlap.

To summarize, purely geometric criteria, the ligand size as well as the interface cavity geometry or volume, were shown to be major criteria to discriminate agonists and antagonist interactions. Comparison between docking scores, volume, and cavity overlap suggested the latter criterion could be a useful discriminative tool.

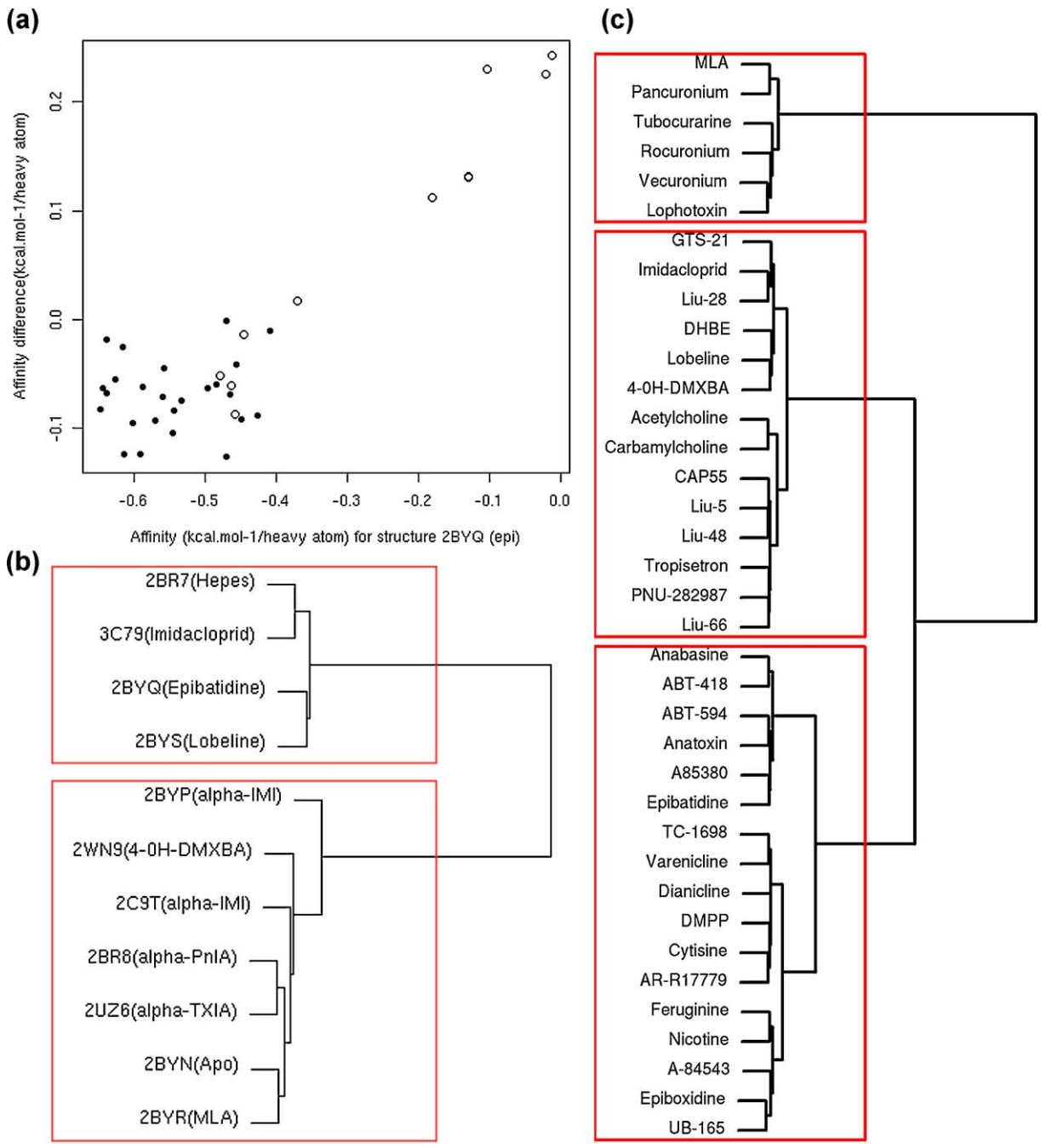

Fig. 3. (a) Plot of the affinity difference (2BYQ-2BYR) as a function of the affinity for the structure 2BYQ (obtained in the presence of epibatidine) for agonists (black bullets) and antagonists (white bullets). Affinity is the Autodock score per heavy atom. (b) Clustering of *Aplysia* AChBP structures based on the RMSD of their binding energy (Autodock score) profiles for all nAChR ligands. (c) Clustering of nAChR ligands based on the RMSD of their binding energy (Autodock score) profiles for all *Aplysia* AChBP structures.

4. Discussion

4.1. Applicability of the presented protocol to other systems

The results presented here show a useful trend. Contrary to previous studies aimed at analyzing in details the interactions of nicotinic compounds with nAChRs [36,71] or AChBP [45], our approach was intended to be compatible with virtual screening protocols and therefore does not require any computationally expensive operations in preparing the ligand or running the docking. Interestingly, it offers good results in terms of comparison to experiments (Fig. 2), although the results have been obtained using substantial simplifications. Indeed, the protein was kept rigid, and the Autodock force field was used, which does not include explicitly the cation–π interaction specific of many nAChR ligands. Moreover, other subtle effects, as the difference in affinity between GTS21 and 4OH-DMXBA, seen experimentally (Supplementary Table 2), cannot be reproduced with the current protocol (Fig. 2). Another advantage of the presented protocol is its straightforward extension to other types of ligands, such as antagonists (e.g. Lophotoxin) and allosteric effectors, and to other members of the LGIC family.

4.2. Distinction of agonists from antagonists in drug design

nAChR antagonists have been proposed to hold therapeutic promise [72] and have indeed been suggested for the treatment

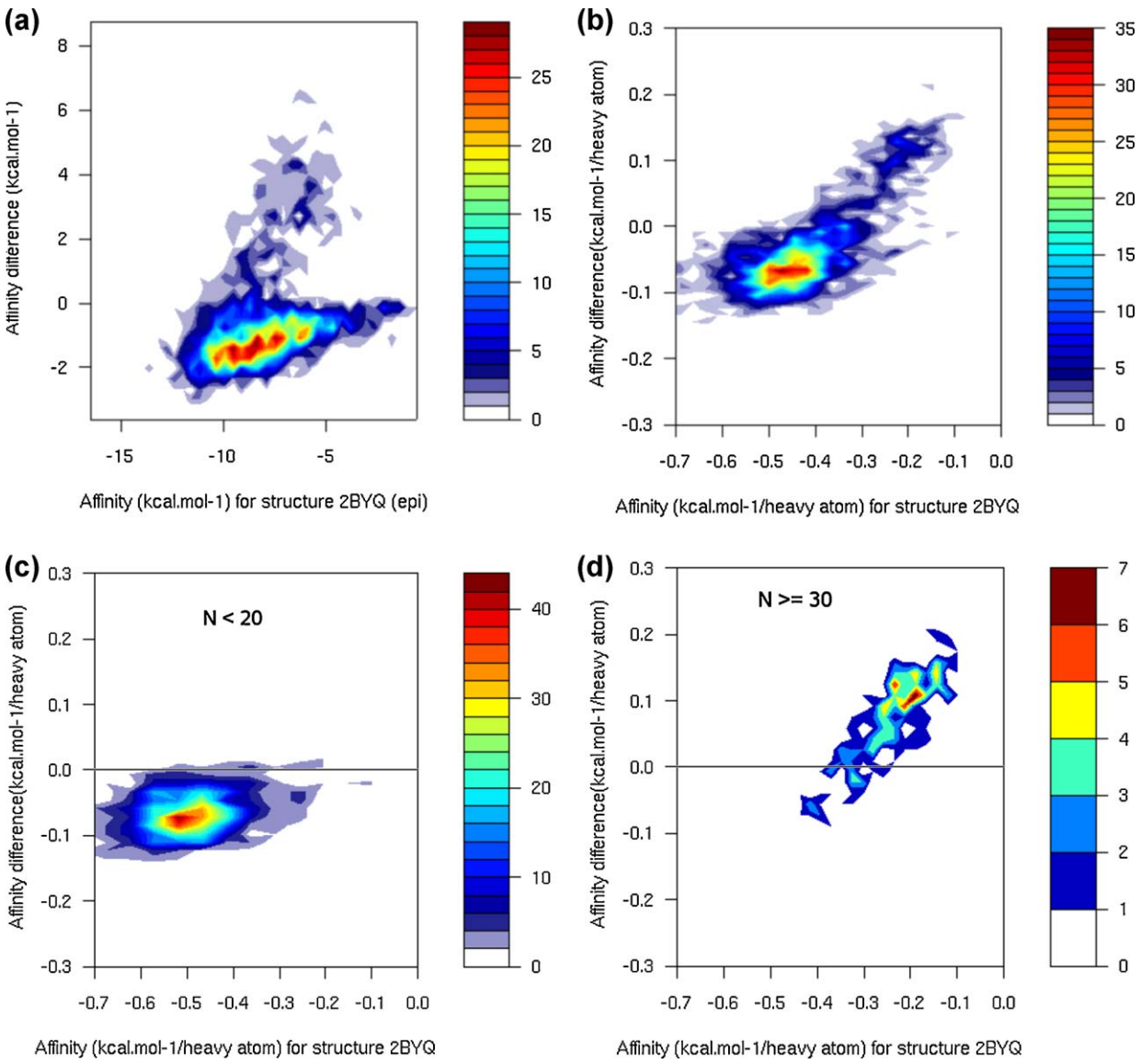

Fig. 4. Docking of the NCI diversity set. Plots of the affinity difference (2BYQ-2BYR) as a function of the affinity for the structure 2BYQ (obtained in the presence of epibatidine). Affinity is expressed in kcal mol^{-1} (a) and corrected for the size of the compound, kcal mol^{-1}/heavy atom (b). Plots of the affinity difference (2BYQ-2BYR) as a function of the affinity for the structure 2BYQ for molecules smaller than 20 heavy atoms (c), and larger than 30 heavy atoms (d).

of non-small cell lung cancer [73] but the discovery of agonists is the main therapeutic goal in targeting nAChRs [3]. Therefore, it is important to differentiate between agonists and antagonists in a drug design project. Indeed, medicinal chemistry effort targeted towards the nAChR, aiming at developing agonists, often result in the preparation of antagonists.

The results described above constitute a useful proof of principle that docking can help to discriminate ligands as a function of their affinity (agonist versus antagonist). Concomitantly, as rationalized by the classification of the cavities located at the interfaces, the choice of template protein structures for virtual screening campaigns appears crucial to favour the discovery of either agonists or antagonists.

In AChBP structures, the C-loop does not display exclusively open and closed positions, but also intermediate ones. Although this aspect is not explicitly taken into account in our analysis, intermediate structures are included in the study as 2BYR considered as intermediate in Bourne et al. [17]. Interestingly open-C-loop structures, although heterogeneous, can be clustered together on the basis of the docking score. This suggests that docking results capture more than just the opening of the C-loop.

Compound size appeared to be the main criteria for classification based on docking score. This was true for nicotinic compounds as well as for the NCI diversity set used as a control. The effect of compound size in the NCI diversity set reveals that the discrimination by the size does not necessarily imply a correct modelling of the ligand specificity.

However, as expected, the ligand size is not the only factor and other criteria must play a role [44]. The case of lobeline is worth mentioning in that context, as several contrasted experimental properties were reported for this molecule. Lobeline was shown to have an agonist effect by electrophysiology experiments on $\alpha4\beta2$ and $\alpha4\beta4$ nAChRs [74,75]. On the other hand, binding experiments have shown that lobeline has atypical properties for an agonist [76] and antagonistic properties of lobeline (and nicotine) were observed at the neuromuscular junction [77]. In the present study, lobeline, the largest nAChR agonist with 25 heavy atoms, was classified with weak agonists and small antagonists. Furthermore, as observed in this study, the cavity overlap appears as a better

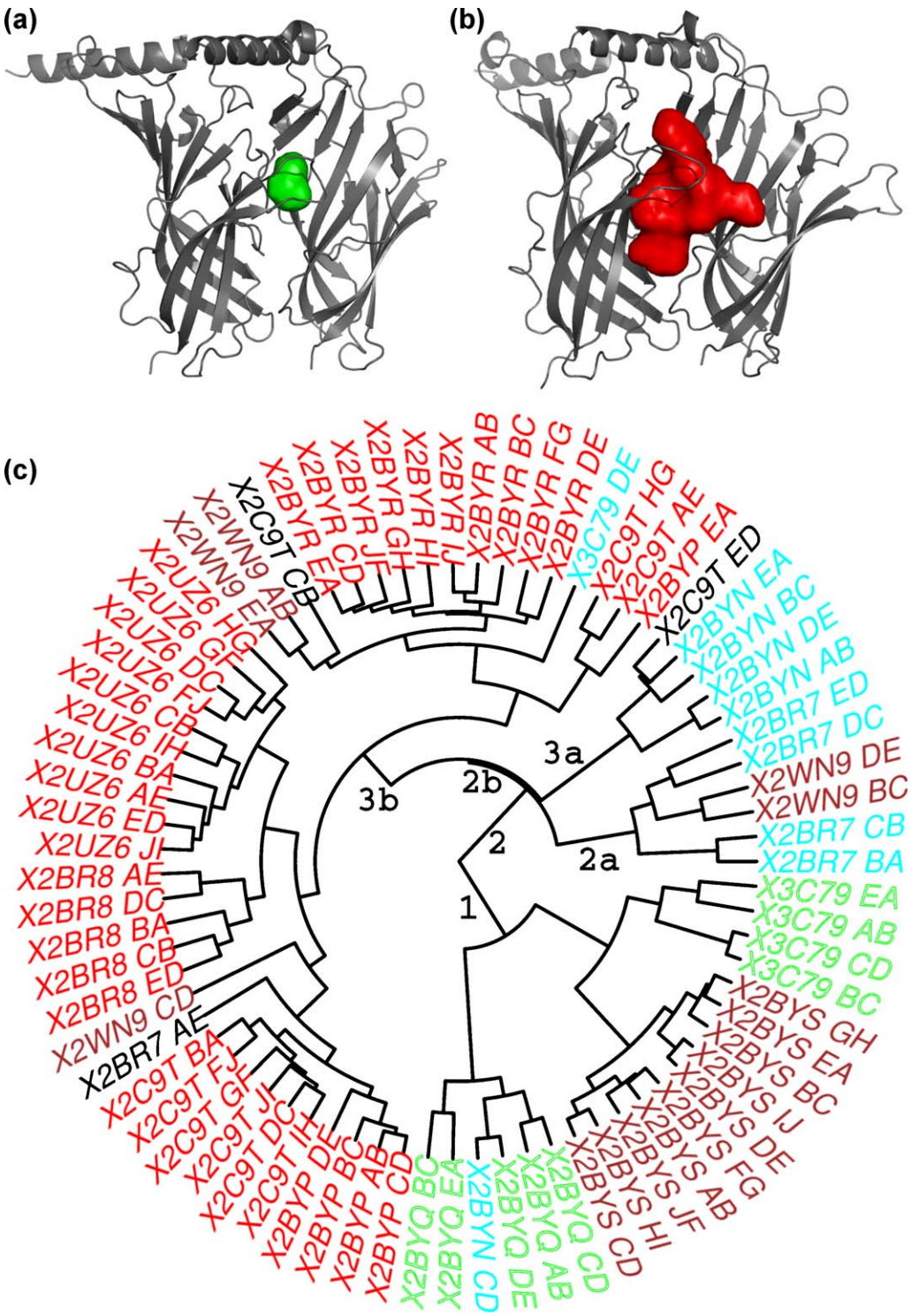

Fig. 5. Analysis of interface cavities in AChBP dimers extracted from X-ray crystallographic structures. (a and b) Geometric cavities detected at the interface of subunits. The surface of the grid points defining the cavities is displayed and the two dimers are coloured in grey. (a) Dimer from 2BYQ complexed with an agonist (epibatidine), the cavity is coloured in green, (b) dimer from 2BYR complexed with an antagonist (MLA), the cavity is coloured in red (c). Phylogenic tree of the AChBP dimer X-ray crystallographic structures generated from the hierarchical clustering based on the superposition of interface cavities. The dimer interface names (PDB entry concatenated with the dimer chains id) are coloured according to the type of bound ligand (green: agonist, red: antagonist, brown: partial agonist, black: apo, blue: crystallographic co-factors).

indicator than volume of the cavity only to relate to known ligand score discrimination on various receptor conformation (Fig. 3b and Supplementary Fig. 4). Therefore, the ligand size or cavity volume is not the unique criterion to predict the interaction with nAChRs. The protocol presented here appeared, beyond the effect of ligand size, to be sensitive to the agonist and antagonist properties of the docked ligands.

5. Conclusion

For rational structure based drug design, the choice of the most relevant protein-ligand models is essential. Direct use of AChBP structures has been suggested for drug design projects and, although this choice could be contested [78], it proved fruitful [14]. As the ligand size was shown here to play a major role in the

description of the interaction, a binding site of appropriate volume/size is crucial to select agonist or antagonist and this should orient the selection of AChBP structures used for docking. The protocol presented here can guide the protein template choice, according to the investigated type of ligands. Furthermore, this docking approach can be used to screen large compounds libraries and discriminate between agonists and antagonists.

Appendix A. Supplementary data

Supplementary data associated with this article can be found, in the online version, at doi:10.1016/j.jmgm.2011.06.008.

References

[1] J.-P. Changeux, S.J. Edelstein, Nicotinic Acetylcholine Receptors: From Molecular Biology to Cognition, 1st ed., Odile Jacob, New York, 2005.
[2] J.P. Changeux, S.J. Edelstein, Allosteric mechanisms of signal transduction, Science 308 (2005) 1424–1428.
[3] A. Taly, P.J. Corringer, D. Guedin, P. Lestage, J.P. Changeux, Nicotinic receptors: allosteric transitions and therapeutic targets in the nervous system, Nat. Rev. Drug Discov. 8 (2009) 733–750.
[4] P.J. Corringer, N. Le Novere, J.P. Changeux, Nicotinic receptors at the amino acid level, Annu. Rev. Pharmacol. Toxicol. 40 (2000) 431–458.
[5] G. Wilson, A. Karlin, Acetylcholine receptor channel structure in the resting, open, and desensitized states probed with the substituted-cysteine-accessibility method, Proc. Natl. Acad. Sci. U.S.A. 98 (2001) 1241–1248.
[6] J.P. Changeux, P. Courrege, A. Danchin, J.M. Lasry, A biochemical mechanism for the epigenesis of the neuromuscular junction, C. R. Seances Acad. Sci. III 292 (1981) 449–453.
[7] S.J. Edelstein, O. Schaad, E. Henry, D. Bertrand, J.P. Changeux, A kinetic mechanism for nicotinic acetylcholine receptors based on multiple allosteric transitions, Biol. Cybern. 75 (1996) 361–379.
[8] S.J. Edelstein, O. Schaad, J.P. Changeux, Single binding versus single channel recordings: a new approach to study ionotropic receptors, Biochemistry 36 (1997) 13755–13760.
[9] P. Purohit, A. Auerbach, Unliganded gating of acetylcholine receptor channels, Proc. Natl. Acad. Sci. U.S.A. 106 (2009) 115–120.
[10] K. Brejc, W.J. van Dijk, R.V. Klaassen, M. Schuurmans, J. van Der Oost, A.B. Smit, et al., Crystal structure of an ACh-binding protein reveals the ligand-binding domain of nicotinic receptors, Nature 411 (2001) 269–276.
[11] T.K. Sixma, A.B. Smit, Acetylcholine binding protein (AChBP): a secreted glial protein that provides a high-resolution model for the extracellular domain of pentameric ligand-gated ion channels, Annu. Rev. Biophys. Biomol. Struct. 32 (2003) 311–334.
[12] A.B. Smit, N.I. Syed, D. Schaap, J. van Minnen, J. Klumperman, K.S. Kits, et al., A glia-derived acetylcholine-binding protein that modulates synaptic transmission, Nature 411 (2001) 261–268.
[13] N. Le Novere, T. Grutter, J.P. Changeux, Models of the extracellular domain of the nicotinic receptors and of agonist- and Ca^{2+}-binding sites, Proc. Natl. Acad. Sci. U.S.A. 99 (2002) 3210–3215.
[14] P. Taylor, T.T. Talley, Z. Radic, S.B. Hansen, R.E. Hibbs, J. Shi, Structure-guided drug design: conferring selectivity among neuronal nicotinic receptor and acetylcholine-binding protein subtypes, Biochem. Pharmacol. 74 (2007) 1164–1171.
[15] S. Dutertre, R.J. Lewis, Toxin insights into nicotinic acetylcholine receptors, Biochem. Pharmacol. 72 (2006) 661–670.
[16] R.E. Hibbs, G. Sulzenbacher, J. Shi, T.T. Talley, S. Conrod, W.R. Kem, et al., Structural determinants for interaction of partial agonists with acetylcholine binding protein and neuronal alpha7 nicotinic acetylcholine receptor, Embo J. 28 (2009) 3040–3051.
[17] Y. Bourne, Z. Radic, R. Araoz, T.T. Talley, E. Benoit, D. Servent, et al., Structural determinants in phycotoxins and AChBP conferring high affinity binding and nicotinic AChR antagonism, Proc. Natl. Acad. Sci. U.S.A. 107 (2010) 6076–6081.
[18] A. Taly, P.J. Corringer, T. Grutter, L.P. de Carvalho, M. Karplus, J.P. Changeux, Implications of the quaternary twist allosteric model for the physiology and pathology of nicotinic acetylcholine receptors, Proc. Natl. Acad. Sci. U.S.A. 103 (2006) 16965–16970.
[19] A.O. Samson, M. Levitt, Inhibition mechanism of the acetylcholine receptor by alpha-neurotoxins as revealed by normal-mode dynamics, Biochemistry 47 (2008) 4065–4070.
[20] M. Yi, H. Tjong, H.X. Zhou, Spontaneous conformational change and toxin binding in alpha7 acetylcholine receptor: insight into channel activation and inhibition, Proc. Natl. Acad. Sci. U.S.A. 105 (2008) 8280–8285.
[21] X. Cheng, H. Wang, B. Grant, S.M. Sine, J.A. McCammon, Targeted molecular dynamics study of c-loop closure and channel gating in nicotinic receptors, PLoS Comput. Biol. (2006) 2.
[22] A. Taly, J.P. Changeux, Functional organization and conformational dynamics of the nicotinic receptor: a plausible structural interpretation of myasthenic mutations, Ann. N.Y. Acad. Sci. 1132 (2008) 42–52.
[23] X. Liu, Y. Xu, X. Wang, F.J. Barrantes, H. Jiang, Unbinding of nicotine from the acetylcholine binding protein: steered molecular dynamics simulations, J. Phys. Chem. B 112 (2008) 4087–4093.
[24] P.H. Celie, S.E. van Rossum-Fikkert, W.J. van Dijk, K. Brejc, A.B. Smit, T.K. Sixma, Nicotine and carbamylcholine binding to nicotinic acetylcholine receptors as studied in AChBP crystal structures, Neuron 41 (2004) 907–914.
[25] P.H. Celie, I.E. Kasheverov, D.Y. Mordvintsev, R.C. Hogg, P. van Nierop, R. van Elk, et al., Crystal structure of nicotinic acetylcholine receptor homolog AChBP in complex with an alpha-conotoxin PnIA variant, Nat. Struct. Mol. Biol. 12 (2005) 582–588.
[26] S.B. Hansen, G. Sulzenbacher, T. Huxford, P. Marchot, P. Taylor, Y. Bourne, Structures of Aplysia AChBP complexes with nicotinic agonists and antagonists reveal distinctive binding interfaces and conformations, Embo J. 24 (2005) 3635–3646.
[27] Y. Bourne, T.T. Talley, S.B. Hansen, P. Taylor, P. Marchot, Crystal structure of a Cbtx-AChBP complex reveals essential interactions between snake alpha-neurotoxins and nicotinic receptors, Embo J. 24 (2005) 1512–1522.
[28] V. Costa, A. Nistri, A. Cavalli, P. Carloni, A structural model of agonist binding to the alpha3beta4 neuronal nicotinic receptor, Br. J. Pharmacol. 140 (2003) 921–931.
[29] B. Iorga, D. Herlem, E. Barre, C. Guillou, Acetylcholine nicotinic receptors: finding the putative binding site of allosteric modulators using the "blind docking" approach, J. Mol. Model. 12 (2006) 366–372.
[30] T. Grutter, N. Le Novere, J.P. Changeux, Rational understanding of nicotinic receptors drug binding, Curr. Top. Med. Chem. 4 (2004) 645–650.
[31] R.H. Henchman, H.L. Wang, S.M. Sine, P. Taylor, J.A. McCammon, Ligand-induced conformational change in the alpha7 nicotinic receptor ligand binding domain, Biophys. J. 88 (2005) 2564–2576.
[32] R.J. Law, R.H. Henchman, J.A. McCammon, A gating mechanism proposed from a simulation of a human alpha7 nicotinic acetylcholine receptor, Proc. Natl. Acad. Sci. U.S.A. 102 (2005) 6813–6818.
[33] Y. Xu, F.J. Barrantes, X. Luo, K. Chen, J. Shen, H. Jiang, Conformational dynamics of the nicotinic acetylcholine receptor channel: a 35-ns molecular dynamics simulation study, J. Am. Chem. Soc. 127 (2005) 1291–1299.
[34] M. Schapira, R. Abagyan, M. Totrov, Structural model of nicotinic acetylcholine receptor isotypes bound to acetylcholine and nicotine, BMC Struct. Biol. 2 (2002) 1.
[35] S.M. Sine, The nicotinic receptor ligand binding domain, J. Neurobiol. 53 (2002) 431–446.
[36] X. Huang, F. Zheng, C. Stokes, R.L. Papke, C.G. Zhan, Modeling binding modes of alpha7 nicotinic acetylcholine receptor with ligands: the roles of Gln117 and other residues of the receptor in agonist binding, J. Med. Chem. 51 (2008) 6293–6302.
[37] K. Toshima, S. Kanaoka, A. Yamada, K. Tarumoto, M. Akamatsu, D.B. Sattelle, et al., Combined roles of loops C and D in the interactions of a neonicotinoid insecticide imidacloprid with the alpha4beta2 nicotinic acetylcholine receptor, Neuropharmacology 56 (2009) 264–272.
[38] E. Luttmann, J. Ludwig, A. Hoffle-Maas, M. Samochocki, A. Maelicke, G. Fels, Structural model for the binding sites of allosterically potentiating ligands on nicotinic acetylcholine receptors, ChemMedChem 4 (2009) 1874–1882.
[39] M. Parthiban, M.B. Rajasekaran, S. Ramakumar, P. Shanmughavel, Molecular modeling of human pentameric alpha(7) neuronal nicotinic acetylcholine receptor and its interaction with its agonist and competitive antagonist, J. Biomol. Struct. Dyn. 26 (2009) 535–547.
[40] R.X. Gu, H. Gu, Z.Y. Xie, J.F. Wang, H.R. Arias, D.Q. Wei, et al., Possible drug candidates for Alzheimer's disease deduced from studying their binding interactions with alpha7 nicotinic acetylcholine receptor, Med. Chem. 5 (2009) 250–262.
[41] Z.J. Hu, L. Bai, Y. Tizabi, W. Southerland, Computational modeling study of human nicotinic acetylcholine receptor for developing new drugs in the treatment of alcoholism, Interdiscipl. Sci. 1 (2009) 254–262.
[42] B. Tasso, C. Canu Boido, E. Terranova, C. Gotti, L. Riganti, F. Clementi, et al., Synthesis, binding, and modeling studies of new cytisine derivatives, as ligands for neuronal nicotinic acetylcholine receptor subtypes, J. Med. Chem. 52 (2009) 4345–4357.
[43] E. Soriano, J. Marco-Contelles, I. Colmena, L. Gandia, Computational analysis of the binding ability of heterocyclic and conformationally constrained epibatidine analogs in the neuronal nicotinic acetylcholine receptor, Mol. Divers. 14 (2010) 201–211.
[44] X. Huang, F. Zheng, C.G. Zhan, Modeling differential binding of alpha4beta2 nicotinic acetylcholine receptor with agonists and antagonists, J. Am. Chem. Soc. 130 (2008) 16691–16696.
[45] M.A. Turabekova, B.F. Rasulev, F.N. Dzhakhangirov, D. Leszczynska, J. Leszczynski, Aconitum and Delphinium alkaloids of curare-like activity. QSAR analysis and molecular docking of alkaloids into AChBP, Eur. J. Med. Chem. 45 (2010) 3885–3894.
[46] F. Gao, N. Bern, A. Little, H.L. Wang, S.B. Hansen, T.T. Talley, et al., Curariform antagonists bind in different orientations to acetylcholine-binding protein, J. Biol. Chem. 278 (2003) 23020–23026.
[47] J.A. Abin-Carriquiry, M.P. Zunini, B.K. Cassels, S. Wonnacott, F. Dajas, In silico characterization of cytisinoids docked into an acetylcholine binding protein, Bioorg. Med. Chem. Lett. 20 (2010) 3683–3687.
[48] S.H. Slavov, M. Radzvilovits, S. LeFrancois, I.B. Stoyanova-Slavova, F. Soti, W.R. Kem, et al., A computational study of the binding of 3-(arylidene) anabaseines to two major brain nicotinic acetylcholine receptors and to the acetylcholine binding protein, Eur. J. Med. Chem. 45 (2010) 2433–2446.

[49] M. Utsintong, T.T. Talley, P.W. Taylor, A.J. Olson, O. Vajragupta, Virtual screening against alpha-cobratoxin, J. Biomol. Screen. 14 (2009) 1109–1118.
[50] A. Babakhani, T.T. Talley, P. Taylor, J.A. McCammon, A virtual screening study of the acetylcholine binding protein using a relaxed-complex approach, Comput. Biol. Chem. 33 (2009) 160–170.
[51] C. Ulens, A. Akdemir, A. Jongejan, R. van Elk, S. Bertrand, A. Perrakis, et al., Use of acetylcholine binding protein in the search for novel alpha7 nicotinic receptor ligands. In silico docking, pharmacological screening, and X-ray analysis, J. Med. Chem. 52 (2009) 2372–2383.
[52] R. Artali, G. Bombieri, F. Meneghetti, Docking of 6-chloropyridazin-3-yl derivatives active on nicotinic acetylcholine receptors into molluscan acetylcholine binding protein (AChBP), Farmaco 60 (2005) 313–320.
[53] S.M. Sine, H.L. Wang, F. Gao, Toward atomic-scale understanding of ligand recognition in the muscle nicotinic receptor, Curr. Med. Chem. 11 (2004) 559–567.
[54] M. Konstantakaki, J. Changeux, A. Taly, Docking of long chain alpha-cobratoxin suggests a basal state conformation of the nicotinic receptor, Biochem. Biophys. Res. Commun. 359 (2007) 413–418.
[55] E.J Haddadian, M.H. Cheng, R.D. Coalson, Y. Xu, P. Tang, In silico models for the human alpha4beta2 nicotinic acetylcholine receptor, J. Phys. Chem. B 112 (2008) 13981–13990.
[56] H. Zhang, H. Li, Q. Ma, QSAR study of a large set of 3-pyridyl ethers as ligands of the alpha4beta2 nicotinic acetylcholine receptor, J. Mol. Graph. Model. 26 (2007) 226–235.
[57] T. Sander, A.T. Bruun, T. Balle, Docking to flexible nicotinic acetylcholine receptors: a validation study using the acetylcholine binding protein, J. Mol. Graph. Model. (2010).
[58] G.M. Morris, D.S. Goodsell, R.S. Halliday, R. Huey, W.E. Hart, R.K. Belew, et al., Automated docking using a lamarckian genetic algorithm and an empirical binding free energy function, J. Comput. Chem. 19 (1998) 1639–1662.
[59] C. Ulens, R.C. Hogg, P.H. Celie, D. Bertrand, V. Tsetlin, A.B. Smit, et al., Structural determinants of selective alpha-conotoxin binding to a nicotinic acetylcholine receptor homolog AChBP, Proc. Natl. Acad. Sci. U.S.A. 103 (2006) 3615–3620.
[60] T.T. Talley, M. Harel, R.E. Hibbs, Z. Radic, M. Tomizawa, J.E. Casida, et al., Atomic interactions of neonicotinoid agonists with AChBP: molecular recognition of the distinctive electronegative pharmacophore, Proc. Natl. Acad. Sci. U.S.A. 105 (2008) 7606–7611.
[61] S. Dutertre, C. Ulens, R. Buttner, A. Fish, R. van Elk, Y. Kendel, et al., AChBP-targeted alpha-conotoxin correlates distinct binding orientations with nAChR subtype selectivity, Embo J. 26 (2007) 3858–3867.
[62] J. Liu, J.B. Eaton, B. Caldarone, R.J. Lukas, A.P. Kozikowski, Chemistry and pharmacological characterization of novel nitrogen analogues of AMOP-H-OH (sazetidine-A, 6-[5-(azetidin-2-ylmethoxy)pyridin-3-yl]hex-5-yn-1-ol) as alpha4beta2-nicotinic acetylcholine receptor-selective partial agonists, J. Med. Chem. 53 (2010) 6973–6985.
[63] N. Zaveri, F. Jiang, C. Olsen, W. Polgar, L. Toll, Novel alpha3beta4 nicotinic acetylcholine receptor-selective ligands. Discovery, structure-activity studies, and pharmacological evaluation, J. Med. Chem. 53 (2010) 8187–8191.
[64] A.D. McLachlan, Rapid comparison of protein structres, Acta Crystallogr. (1982) 871–873.
[65] M.C. Surles, J.S. Richardson, D.C. Richardson, F.P. Brooks Jr., Sculpting proteins interactively: continual energy minimization embedded in a graphical modeling system, Protein Sci. 3 (1994) 198–210.
[66] S.B. Hansen, P. Taylor, Galanthamine and non-competitive inhibitor binding to ACh-binding protein: evidence for a binding site on non-alpha-subunit interfaces of heteromeric neuronal nicotinic receptors, J. Mol. Biol. 369 (2007) 895–901.
[67] S.B. Hansen, T.T. Talley, Z. Radic, P. Taylor, Structural and ligand recognition characteristics of an acetylcholine-binding protein from *Aplysia californica*, J. Biol. Chem. 279 (2004) 24197–24202.
[68] A. Nasiripourdori, V. Taly, T. Grutter, A. Taly, From toxins targeting ligand gated ion channels to therapeutic molecules, Toxins 3 (2011) 260–293.
[69] D. Bertrand, A. Devillers-Thiery, F. Revah, J.L. Galzi, N. Hussy, C. Mulle, et al., Unconventional pharmacology of a neuronal nicotinic receptor mutated in the channel domain, Proc. Natl. Acad. Sci. U.S.A. 89 (1992) 1261–1265.
[70] F. Gao, N. Bren, T.P. Burghardt, S. Hansen, R.H. Henchman, P. Taylor, et al., Agonist-mediated conformational changes in acetylcholine-binding protein revealed by simulation and intrinsic tryptophan fluorescence, J. Biol. Chem. 280 (2005) 8443–8451.
[71] X. Huang, F. Zheng, P.A. Crooks, L.P. Dwoskin, C.G. Zhan, Modeling multiple species of nicotine and deschloroepibatidine interacting with alpha4beta2 nicotinic acetylcholine receptor: from microscopic binding to phenomenological binding affinity, J. Am. Chem. Soc. 127 (2005) 14401–14414.
[72] L.P. Dwoskin, P.A. Crooks, Competitive neuronal nicotinic receptor antagonists: a new direction for drug discovery, J. Pharmacol. Exp. Ther. 298 (2001) 395–402.
[73] P. Russo, A. Catassi, A. Cesario, D. Servent, Development of novel therapeutic strategies for lung cancer: targeting the cholinergic system, Curr. Med. Chem. 13 (2006) 3493–3512.
[74] Q. Liu, K.W. Yu, Y.C. Chang, R.J. Lukas, J. Wu, Agonist-induced hump current production in heterologously-expressed human alpha4beta2-nicotinic acetylcholine receptors, Acta Pharmacol. Sin. 29 (2008) 305–319.
[75] J. Wu, Q. Liu, K. Yu, J. Hu, Y.P. Kuo, M. Segerberg, et al., Roles of nicotinic acetylcholine receptor beta subunits in function of human alpha4-containing nicotinic receptors, J. Physiol. 576 (2006) 103–118.
[76] L.P. Dwoskin, P.A. Crooks, A novel mechanism of action and potential use for lobeline as a treatment for psychostimulant abuse, Biochem. Pharmacol. 63 (2002) 89–98.
[77] R.L. Volle, L. Reynolds, Receptor desensitization by lobeline and nicotine, Naunyn-Schmiedeberg's Arch. Pharmacol. 276 (1973) 49–54.
[78] T. Grutter, L. Prado de Carvalho, D. Virginie, A. Taly, M. Fischer, J.P. Changeux, A chimera encoding the fusion of an acetylcholine-binding protein to an ion channel is stabilized in a state close to the desensitized form of ligand-gated ion channels, C. R. Biol. 328 (2005) 223–234.
[79] A. Gordon, Classification, 2nd ed., Boca Raton, 1999.
[80] R Development Core Team, R: A Language and Environment for Statistical Computing, R Foundation for Statistical Computing, Vienna, Austria, 2006, ISBN 3-900051-07-0, http://www.R-project.org.
[81] A.C.R. Martin, C.T. Porter, http://www.bioinf.org.uk/software/profit/.